Produced Water Workshop
7 – 8 June 2016

Technical Paper

Performance of a Coalescing Multistage Centrifugal Produced Water Pump with Respect to Water Characteristics and Point of Operation

Rune Husveg, University of Agder
Trygve Husveg, Typhonix AS
Niels van Teeffelen, Typhonix AS
Morten Ottestad, University of Agder
Michael R. Hansen, University of Agder

1 ABSTRACT

In this paper, the coalescing effect of a new pump type is investigated with respect to the point of operation and water characteristics. Laboratory testing of the pump has been performed with synthetic produced water containing stabilised crude oil. The coalescing effect was studied by comparing the droplet size distribution at the inlet and outlet of the pump using online measurements. This study was performed for different combinations of inlet droplet size distribution, oil concentration, oil type, flow rate and pumping pressure. For given water characteristics and flow rate, a point of maximum growth of the volume median droplet size (Dv_{50}), with respect to the pumping pressure, was found. These observations are discussed based on turbulent droplet coalescence and droplet break-up theory. It is also exemplified how this knowledge can be used to maximise the potential of the coalescing pump with respect to the efficiency of the downstream separation equipment in a real produced water process.

2 INTRODUCTION

During oil production, water is produced along with the hydrocarbon mixture. The produced water contains a combination of organic and inorganic materials, and must be cleaned before it is discharged into the sea or reinjected into a reservoir [1], [2].

The produced water and gas are separated from the crude oil in large three–phase separators [3]. Produced water treatment methods, based on gravitation, enhanced gravitation, and flotation technologies are used to remove the remaining oil from the water [4]. These methods are based on oil droplet buoyancy, and the efficiency is therefore highly dependent on the diameter of the oil droplets [4]. If the inlet droplet size is increased, it will lead to improved separation efficiency [5].

Hydrocyclones and other produced water treatment equipment normally require a certain feed pressure to operate. Therefore, if the process pressure is too low, pumps are needed to increase the pressure. To avoid reduction of the separation efficiency, droplet break-up should be kept to a minimum. This can be achieved by selecting a pump with minimum shearing of the oil droplets [6]. Flanigan et al. [7] investigated and rated seven different pumps, based on shearing, using droplet size analysis. The pumps represented five different generic types and were ranked from 1 to 5, where 1 was best, and 5 was poorest. The following ranking was presented: (1) progressive cavity pumps, (2) twin lobe pumps, (3) sliding rotary vane pumps, (4) single stage centrifugal pumps, and (5) twin screw pumps. This investigation rated single stage centrifugal pumps as the second worst pump type

regarding droplet shearing. Schubert [8] reported, however, that using a correctly designed centrifugal pump could be a cost effective low shear solution. Recently, van Teeffelen [9] presented results from the prototype testing of a coalescing multistage centrifugal pump. This pump is meant to increase, rather than reduce, the average droplet size. During the testing, the droplet behaviour in the coalescing pump was compared with that of an eccentric screw pump (progressive cavity pump) and a single stage centrifugal pump. The pumps were tested with respect to the volume median droplet diameter (Dv_{50}) at the outlet. The test was performed with small and large inlet droplets (Dv_{50} = 6 - 7 µm and Dv_{50} = 10 - 12 µm) in low and high concentrations (C_{oil} = 100 ppm and C_{oil} = 500 ppm) of light and heavy crude (°API = 44 and °API = 19). The results showed that both the coalescing pump and the eccentric screw pump increased Dv_{50} while the single stage centrifugal pump reduced Dv_{50}. Further, the increase of Dv_{50} in the coalescing pump turned out to be up to four times greater compared to that of the eccentric screw pump for the same conditions. It was also concluded that the coalescing effect of the prototype pump was increased when 1) the oil concentration was increased and 2) Dv_{50} at the inlet was reduced.

This paper will present results from continued investigations of this coalescing centrifugal pump. The coalescing effect will be investigated when adjusting the pumping pressure for different water characteristics and flow rates. The observations will be discussed in the context of known theory for turbulent droplet coalescence and droplet break-up. Also, a method to exploit the process benefits of the pump will be suggested.

3 THEORY

The physics associated with the droplet size development inside the pump are complex and probably require extensive numerical analyses to be predicted, if possible. However, it does seem plausible that two different mechanisms are present at the same time. These are turbulent droplet coalescence and droplet break-up.

3.1 Droplet Coalescence

According to van der Zande [10], the coalescence process in a turbulent flow can be divided into the following two sub-processes: 1) collision of droplets and 2) drainage of the fluid film between them. Among other parameters, the coalescence of droplets is governed by the intensity of the turbulence, the number and size of the droplets, and fluid properties such as viscosity, density, and interfacial tension. Eq. 1 shows the collision frequency for equally sized droplets in the inertial subrange of turbulence. This equation determines how often two droplets collide [10].

$$\omega_{col} = \left(\frac{32\pi}{3}\right)^{1/2} \cdot (\varepsilon \cdot d)^{1/3} \cdot d^2 \cdot n \qquad (1)$$

In Eq. 1, *n* is the number of droplets of diameter *d* per unit volume. *ε* is the energy dissipation per unit mass, which is a measure of the turbulence intensity [11]. As seen from Eq. 1, the collision frequency increases if the number of droplets, the size of the droplets or the turbulence intensity increases. Next, whether a collision leads to coalescence is determined by the coalescence probability. The probability is given by the time it takes to drain the fluid film and the interaction time [10].

This paper will use the collision frequency as an indicator for the coalescence behaviour of the pump. The amount of time turbulence is present is also an important factor for the total number of collisions. In this case, this is the amount of time it takes for a droplet to travel through the pump (residence time).

3.2 Droplet Break-up

For a droplet to break apart, it has to be deformed. Thus, the deforming stress has to be higher than the restoring stress [10], [11]. Several models for the largest stable droplet size in a turbulent flow have been suggested based on a critical ratio between the deforming and the restoring stresses [10], [12]. Morales et al. [13] developed a mechanistic model for the droplet formation through a centrifugal pump. This model was based on turbulent droplet break-up, and Eq. 2 was used as a basis.

$$d_{max} = We_{CRIT}^{3/5} \cdot \left[\frac{\sigma}{\rho_c} + \frac{\sqrt{2}}{4} \cdot \frac{\mu_D \cdot (\varepsilon \cdot d_{max})^{1/3}}{\rho_c} \right]^{3/5} \cdot \varepsilon^{-2/5} \qquad (2)$$

In Eq. 2, We_{CRIT} is the critical Weber number, σ is the interfacial tension, ρ_c is the density of the continuous phase, μ_D is the viscosity of the dispersed phase, and d_{max} is the largest stable droplet diameter. Morales et al. [13] approximated the turbulent energy dissipation rate per unit mass through the centrifugal pump as follows:

$$\varepsilon = \kappa \cdot \frac{\Delta p \cdot Q_m}{\rho_m \cdot V_{VOLUTE}} \qquad (3)$$

In Eq. 3, κ is a proportional constant, Δp is the pumping pressure, Q_m and ρ_m are the flow rate and density of the oil/water mixture, and V_{VOLUTE} is the volume of the pump volute. As pointed out by Morales et al. [13], if the viscous stress in Eq. 2 can be neglected compared to the interfacial stress, it implies that $d_{max} \propto \varepsilon^{-0.4}$. On the other hand, if the interfacial stress is negligible, then $d_{max} \propto \varepsilon^{-0.2}$. Therefore, $d_{max} \propto \varepsilon^{\alpha}$, where α varies from -0.2 (viscous stress dominant) to -0.4 (interfacial stress dominant). If κ, ρ_m, V_{VOLUTE}, ρ_c, μ_D, σ and We_{CRIT} are assumed to be constant, then a normalised value for the turbulent energy dissipation rate, $\hat{\varepsilon}$, and the maximum stable droplet size, $\hat{d}_{max}$, can be introduced:

$$\hat{\varepsilon} = \frac{\varepsilon}{|\varepsilon^{ref}|} = \frac{\Delta p \cdot Q_m}{|\Delta p^{ref} \cdot Q_m{}^{ref}|} \qquad (4)$$

$$\hat{d}_{max} = \frac{d_{max}}{|d_{max}{}^{ref}|} = \left(\frac{\varepsilon}{|\varepsilon^{ref}|} \right)^{\alpha} = \hat{\varepsilon}^{\alpha} \qquad (5)$$

In this paper, Eq. 4 and Eq. 5 are used to indicate the overall droplet behaviour in the coalescing pump.

4 EXPERIMENTAL SETUP

4.1 Test Rig

Figure 1 gives a schematic representation of the Coalescing Pump Test Rig, which was built specifically for this study. The main test section consisted of 1" piping whereas the supply and return sections consisted of 4" piping and 1" hoses. The oil injection and sampling sections were built with ¼" tubing.

Before testing, water and salt were mixed and heated in the Preparation Tank, T01. The salty water was then circulated through a heat exchanger (not shown in the schematics) until the desired temperature was reached.

During testing, the heated saltwater was pumped from the Preparation Tank, T01, using a centrifugal pump, P01. Flow transmitter FT01 measured the flow rate, Q_{PW}. Crude oil was injected into the saltwater stream to create the synthetic produced water. From the oil injection point, saltwater and oil were directed through hand valve PCV01 (needle valve). The valve was used as a mixing valve, and the opening was adjusted to obtain the desired volume median droplet diameter at the inlet of the Coalescing Pump, Dv_{50in}. The synthetic produced water was then directed through the Coalescing Pump, P02. The speed of the pump was adjusted, using a variable frequency drive, until the desired differential pressure, Δp_{CP}, was achieved. The pressure at the pump inlet and outlet was measured by PT02 and PT03, respectively. The differential pressure across the Coalescing Pump was measured by DP02. The pressure at the inlet of the coalescing pump was set by adjusting hand valve PCV02 (needle valve) and kept constant at p_{in} = 10 bar. During testing, the synthetic produced water was guided towards the Drain Tank, T02, through hand valve HV05 (ball valve). Level transmitter LT02 was used to determine the level in the tank. During commissioning, calibration and testing without oil, the saltwater stream was re-circulated to the Preparation Tank, T01, through hand valve HV04 (ball valve). Samples of the synthetic produced water were fed to the Droplet Analyser either through hand valve HV02 or HV03 (ball valves). HV02 or HV03 was opened when the water characteristic at the inlet or outlet of the Coalescing Pump was analysed. Before the Coalescing Pump was started, the

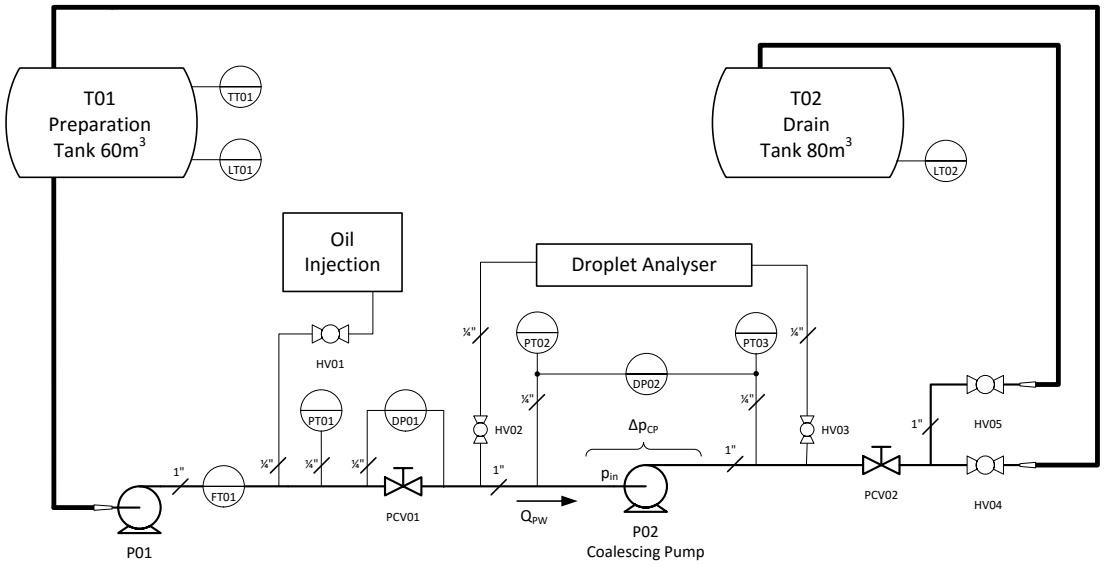

Figure 1 – Schematics of the Coalescing Pump Test Rig.

droplet size distribution was measured at the inlet and outlet of the pump. A slight pressure drop was present as the water went through the non-operating pump. However, these results are referred to as $\Delta p_{CP} = 0$ bar. The Coalescing Pump was thereafter started, and the desired pumping pressure was selected. The inlet and outlet droplets were measured, and the droplet size distributions were averaged over 10 seconds of sampling. PCV01 and PCV02 were adjusted to ensure identical conditions for all tests.

4.2 Test Conditions

In this paper, the term *Point of Operation* is used for the combination of the flow rate through the pump and differential pressure across the pump. The term *Water Characteristic* is used for the combination of droplet size distribution, oil in water concentration and oil type. Water temperature and salinity are also considered as part of the water characteristic. However, these parameters were constant for all tests. The salt concentration was 3.5%, by weight, and the following combination of salts was used: NaCl - 95.9%, $CaCl_2$ - 3.2% and $MgCl_2$ - 0.9%. Further, the saltwater was heated to 49°C ± 1°C.

Stabilised crude oil was used during the testing. The oil was injected into the centre of the pipe through a tube which was bent the same direction as the saltwater flow. Before injection, the oil was heated and stirred to ensure homogeneous conditions in the reservoir. A piston pump was used to pump the oil through an accumulator module which secured a steady flow into the saltwater stream. The manufacturer of the injection pump specifies an accuracy of ± 1% for water over the full flow rate and pressure ranges [14]. As the pumped fluid was crude oil, and therefore has significantly higher viscosity and contains particles, the flow rate was also inspected manually at the beginning of each test period. The concentration of oil in the saltwater was determined based on the oil injection rate and the saltwater flow rate. In this investigation, the following concentrations, C_{oil}, were used: 100, 500, and 1000 ppm. In addition, $C_{oil} = 1500$ ppm was used for one specific test.

Two crude oils were used during the testing and are referred to as *Light Crude* and *Medium Crude*, or according to their °API value. Properties of the crude oils are given in Table 1. The viscosity was measured at a shear rate = 100 s^{-1}.

Table 1 – Properties of the crudes used in the experiments.

Oil Type	°API	Density (kg/m^3)	Viscosity [cP]
Light Crude	44 (60°F)	796 (20°C) 789 (50°C)	2.5 (20°C) 0.5 (50°C)
Medium Crude	27 (60°F)	882 (20°C) 868 (50°C)	27.2 (20°C) 10.7 (50°C)

The light crude had a temperature of 15°C when it was injected into the saltwater stream. However, due to difficulties handling higher viscosities during pumping, the medium crude oil was heated to 50°C. Due to the low concentrations of oil in the water, it is assumed that the droplets of both crudes immediately adapt the temperature of the saltwater [15].

The studied pump, P02, was designed according to the coalescing pump principles developed by Typhonix AS [16]. It is emphasised that the resulting coalescing effect is a design parameter and can vary. However, it is assumed that the overall trends presented in this paper will be the same for any pump design and size.

The coalescing pump was mainly tested for three flow rates; Q_{PW} = 2.5 m^3/h, Q_{PW} = 3.25 m^3/h and Q_{PW} = 4 m^3/h. For each flow rate and water characteristic, the pumping pressure was increased stepwise from Δp_{CP} = 0 bar to Δp_{CP} = 10 bar. All measured parameters were allowed to reach a steady state before being recorded. In one specific test, four additional flow rates were included; Q_{PW} = 1 m^3/h, Q_{PW} = 1.75 m^3/h, Q_{PW} = 4.75 m^3/h and Q_{PW} = 5.5 m^3/h.

4.3 Droplet Size Distribution and Measurement

A Malvern Insitec was used to determine the droplet size distribution. The analyser measures the light scattering pattern in a flow cell and uses Mie theory to determine the droplet sizes [17]. Isokinetic sampling [7] was used to obtain the samples.

The droplet size distribution measurements provided by the droplet analyser are volume based [17]. In this paper Dv_x is defined as the diameter of a droplet where this and all smaller droplets represent x% of the total volume of oil in the distribution. The inlet droplet size distributions used in this investigation are mainly referred to by the size of Dv_{50}.

A typical inlet droplet distribution representing the smallest droplets used in this study, Dv_{50} = 5 µm, is illustrated in Figure 2. This figure shows a bimodal distribution. This type of distribution is typically found where high shearing occurs [18]. Table 2 shows the pressure drop required across the mixing valve for obtaining the different droplet size distributions used in this study. It was observed that the required pressure drop increased as the flow rate was reduced. The values in Table 2 are therefore the average pressure drop based on all combinations of flow rate and oil concentration for each specific droplet size distribution and oil type. A typical distribution containing medium sized droplets, Dv_{50} = 10 µm, is shown in Figure 3. An illustration of a distribution containing the largest droplets, Dv_{50} = 15 µm, is provided in Figure 4. The distributions are presented in two ways. Firstly, the cumulative volume distribution function is showed by a line chart. This chart indicates the percentage volume of droplets having a particular or smaller

Table 2 – Average pressure drop created across PCV01 in order to promote the different inlet droplet size distributions.

Dv_{50in} (µm)	**Light Crude** (bar)	**Medium Crude** (bar)
5	8	10
10	3.4	4
15	2	2.1

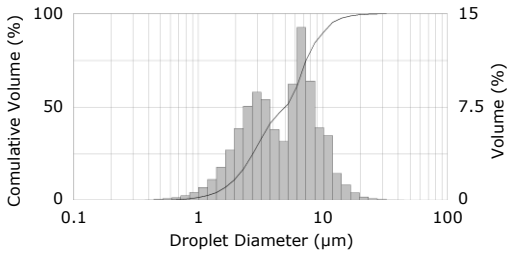

Figure 2 – Typical inlet droplet size distribution with Dv_{50} = 5 µm.

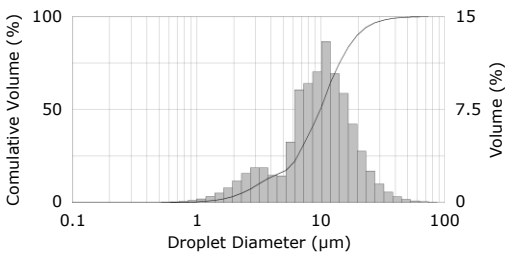

Figure 3 – Typical inlet droplet size distribution with Dv_{50} = 10 µm.

diameter. Dv_{50} is the droplet diameter where the cumulative volume = 50%. Secondly, the distribution is presented in a histogram. This chart shows how volume percentages of the sample distributes within specific size intervals.

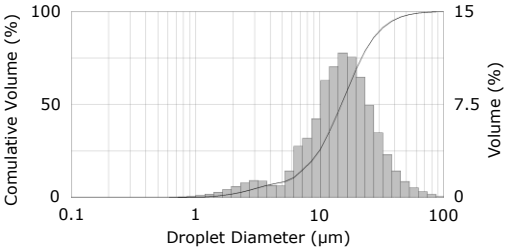

Figure 4 – Typical inlet droplet size distribution with Dv_{50} = 15 µm.

5 RESULTS AND DISCUSSIONS

5.1 Overall Droplet Behaviour

The overall droplet behaviour in the pump was examined in the context of the theory presented in Section 3. During constant water characteristics, the outlet droplet size distribution was measured for different points of operation. According to Eq. 3, this should promote different turbulence intensities inside the pump. Eq. 4 was used to calculate the normalised energy dissipation rate per unit mass. The point of highest turbulence intensity was chosen as a reference. At this operating point, Δp_{CP} = 10 bar and Q_{PW} = 5.5 m^3/h. The simplifications made for Eq. 4 and Eq. 5 are assumed to apply to this test, as the water characteristics were constant. Small droplets of the light crude (Dv_{50in} = 5 µm) in a high concentration (C_{oil} = 1500 ppm) was created upstream from the pump. These conditions were expected to promote a strong coalescing effect [9]. To relate the test results to the theory, Dv_{95} was measured. This value is comparable to the maximum droplet size, d_{max}.

In Figure 5, the x-axis shows the normalised turbulent energy dissipation rate (Eq. 4) for the different points of operation. The left y-axis shows the measured Dv_{95} at the pump outlet. From Figure 2, it was seen that the typical size of Dv_{95} at the pump inlet is 16 µm when Dv_{50in} = 5 µm. The right-hand y-axis in Figure 5 shows the normalised maximum stable droplet size as determined by Eq. 5. α was manually adjusted within the range from -0.4 to -0.2 and determined according to the largest droplets measured in the test. A value of α = -0.32 was chosen. The measured Dv_{95} at Q_{PW} = 5.5 m^3/h and Δp_{CP} = 10 bar was used as a reference for Eq. 5.

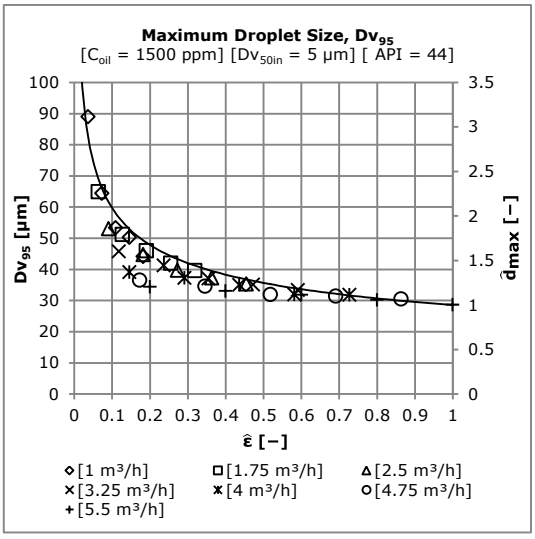

Figure 5 – Measured maximum droplet size (Dv_{95}) and estimated normalised maximum droplet size ($\hat{d}_{max}$) as a function of the normalised turbulent energy dissipation rate ($\hat{\varepsilon}$) for various points of operation.
Dv_{50in} = 5 µm, $Q_{PW} \in \{1, 1.75, 2.5, 3.25, 4, 4.75, 5.5\} m^3/h$, $\Delta p_{CP} \in \{2, 4, 6, 8, 10\}$bar, C_{oil} = 1500 ppm and °API = 44.

Figure 5 clearly indicates the presence of droplet coalescence, as Dv_{95} is increased from 16 µm to 30 - 90 µm. In addition, the size of the largest droplets seems to be restricted to the maximum size approximated by Eq. 5. It is therefore assumed that the overall droplet behaviour in the pump is a combined result of turbulent droplet coalescence and droplet break-up. It is also assumed that the residence time was sufficiently high during all flow rates for some of the droplets to reach the maximum size. This assumption is based on the

observation that Dv_{95} is roughly the same for a constant turbulence intensity, regardless of the flow rate.

In the continuation of this paper, Dv_{50} at the inlet and outlet of the pump are compared, and the percentage change is denoted $\Delta Dv_{50}^{(\%)}$. It is assumed that Dv_{50} gives a better measure of the combined effect of the coalescence and droplet break-up, compared to Dv_{95}. In addition, Dv_{50} is the parameter that is mostly referred to in the oil industry, particularly in produced water applications. Polynomial lines are added to the charts to emphasise the observed trends.

5.2 Effect of Point of Operation

The effect of changing the point of operation was studied with respect to the percentage change of Dv_{50}. Figure 6 shows $\Delta Dv_{50}^{(\%)}$ for various points of operation. In the figure, each curve represents the percentage change of Dv_{50} ($\Delta Dv_{50}^{(\%)}$) for a specific flow rate (Q_{PW}) with respect to the pumping pressure (Δp_{CP}). The water characteristics and points of operation in Figure 6 are identical to those presented in Figure 5.

Figure 6 shows that the point of operation affects the coalescing effect at a constant water characteristic. It is observed that the coalescing effect generally is increased for a reduced flow rate, regardless of the pumping pressure. This observation can be related to the increased residence time. Further, for a constant flow rate, it is seen that the pumping pressure alone affects the coalescing effect. This can be related to the balance of droplet coalescence and droplet break-up. According to Eq. 3, the turbulence intensity is proportional to the pumping pressure during constant flow rate and water characteristics.

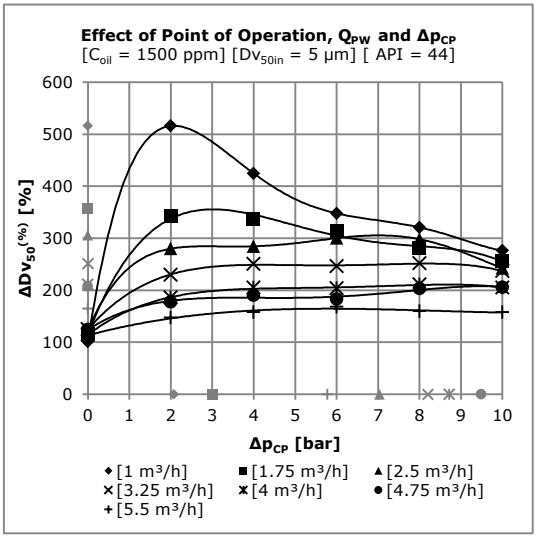

Figure 6 – Percentage change of Dv_{50} ($\Delta Dv_{50}^{(\%)}$) with respect to the pumping pressure (Δp_{CP}) for different flow rates (Q_{PW}).
Dv_{50in} = 5 µm, $Q_{PW} \in \{1, 1.75, 2.5, 3.25, 4, 4.75, 5.5\}$ m³/h, C_{oil} = 1500 ppm and °API = 44.

A point of maximum growth of Dv_{50} is observed with respect to the pumping pressure at each flow rate. It is assumed that this point of operation promotes the most beneficial turbulence intensity with respect to $\Delta Dv_{50}^{(\%)}$, and therefore the best combination of droplet coalescence and break-up. In Figure 6, Δp_{CP} and $\Delta Dv_{50}^{(\%)}$ are respectively projected onto the x- and y-axis at the optimal points of operation. It is observed that the most beneficial Δp_{CP}, with respect to $\Delta Dv_{50}^{(\%)}$, typically increases for an increased Q_{PW}.

Figure 6 shows that, when Q_{PW} = 4 m³/h and Δp_{CP} = 8 bar, $\Delta Dv_{50}^{(\%)} \approx$ 210%. If, however, Q_{PW} is reduced to 1 m³/h while Δp_{CP} is kept at 8 bar, $\Delta Dv_{50}^{(\%)}$ reaches approximately 320%. Next, it can be seen from the graph that Δp_{CP} = 8 bar is not the optimal pumping pressure at Q_{PW} = 1 m³/h. To have an optimal operation, Δp_{CP}

should be reduced from 8 bar to 2 bar. If this adjustment is done, $\Delta Dv_{50}^{(\%)}$ will reach over 510%.

Overall, Figure 6 demonstrates that the point of operation affects the coalescing effect at constant water characteristics. In the continuation, the effects of changes in the water characteristics are studied. In these studies, Q_{PW} is kept constant while Δp_{CP} is changed during various combinations of Dv_{50in}, C_{oil} and oil type.

5.3 Effect of Inlet Droplet Size Distribution

Figure 7 and Figure 8 show results where the Q_{PW} and C_{oil} are kept constant while Dv_{50in} and Δp_{CP} are changed. Figure 7 shows results from the light crude, and Figure 8 shows results from the medium crude.

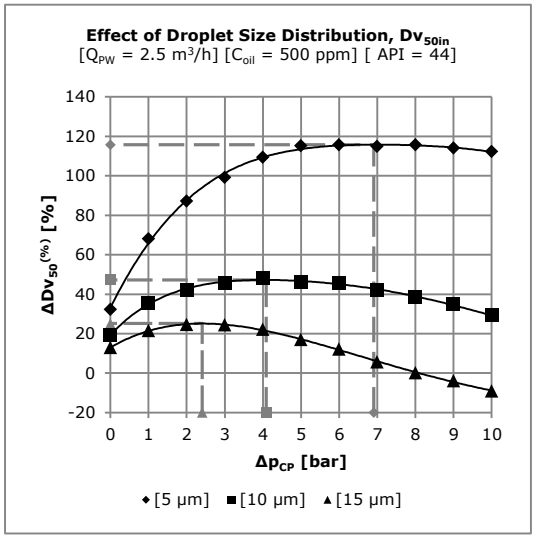

Figure 7 – Percentage change of Dv_{50} ($\Delta Dv_{50}^{(\%)}$) with respect to the pumping pressure (Δp_{CP}) for different inlet droplet size distributions (Dv_{50in}).
$Dv_{50in} \in \{5, 10, 15\}\mu m$, Q_{PW} = 2.5 m^3/h, C_{oil} = 500 ppm and °API = 44.

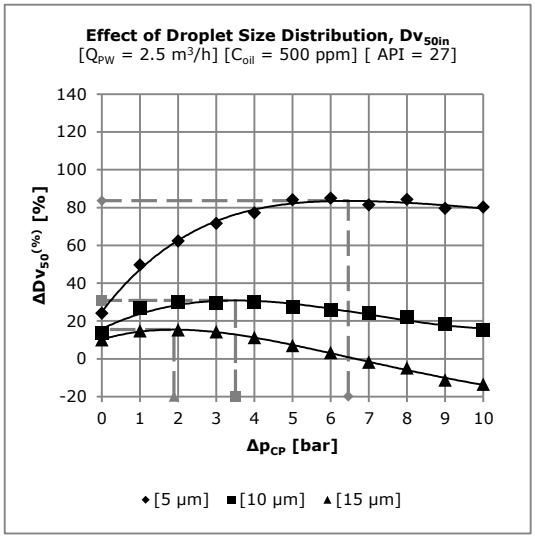

Figure 8 – Percentage change of Dv_{50} ($\Delta Dv_{50}^{(\%)}$) with respect to the pumping pressure (Δp_{CP}) for different inlet droplet size distributions (Dv_{50in}).
$Dv_{50in} \in \{5, 10, 15\}\mu m$, Q_{PW} = 2.5 m^3/h, C_{oil} = 500 ppm and °API = 27.

The results show that a change in the Dv_{50in} affects the coalescing effect. It can be seen that an increased Dv_{50in} leads to a reduced $\Delta Dv_{50}^{(\%)}$, regardless of Δp_{CP}. As C_{oil} is constant in this study, an increased Dv_{50in} reduces the number of droplets. Further, it is observed that this reduces $\Delta Dv_{50}^{(\%)}$. This observation is in accordance with Eq. 1, where a reduced number of droplets reduces the collision frequency. It is also observed that $\Delta Dv_{50}^{(\%)}$ is higher for the light crude compared to the medium crude, at the same conditions. The fluid properties are therefore assumed to affect the coalescence probability and the largest stable droplet size. However, this is not studied further in this paper.

Some of the operational points resulted in negative $\Delta Dv_{50}^{(\%)}$. This was typically observed for high pumping pressure combined with large inlet droplets (Dv_{50in} = 15 µm) and small or medium concentrations (C_{oil} = 100 ppm – 500 ppm). The negative $\Delta Dv_{50}^{(\%)}$ indicates that, for these conditions, the droplet break-up is more intense compared to the coalescence.

Regarding the optimal point of operation, it is seen that the optimal Δp_{CP} decreases for an increased Dv_{50in}. It is assumed that the distribution with a higher Dv_{50in} are more vulnerable to the turbulence intensity as the majority of droplets are closer to the critical size, d_{max}, already before they enter the pump.

Figure 8 shows that $\Delta Dv_{50}^{(\%)} \approx 80\%$ when Dv_{50in} = 5 µm and Δp_{CP} = 6.5 bar. Next, if Dv_{50in} is increased from 5 µm to 15 µm, without any changes in the point of operation, then $\Delta Dv_{50}^{(\%)} \approx 0\%$. In this case, in order to have optimal pumping, Δp_{CP} should be reduced to 2 bar.

5.4 Effect of Oil Concentration

Figure 9 and Figure 10 show results where Q_{PW} and Dv_{50in} are kept constant while C_{oil} and Δp_{CP} are changed.

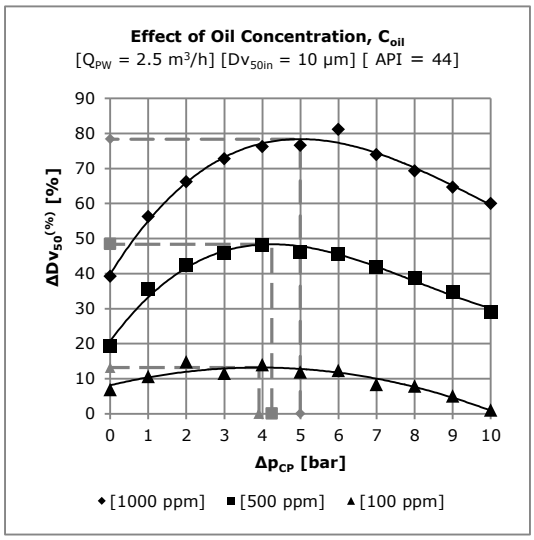

Figure 9 – Percentage change of Dv_{50} ($\Delta Dv_{50}^{(\%)}$) with respect to the pumping pressure (Δp_{CP}) for different oil concentrations (C_{oil}).
Dv_{50in} = 10 µm, Q_{PW} = 2.5 m^3/h, $C_{oil} \in$ {100, 500, 1000}ppm and °API = 44.

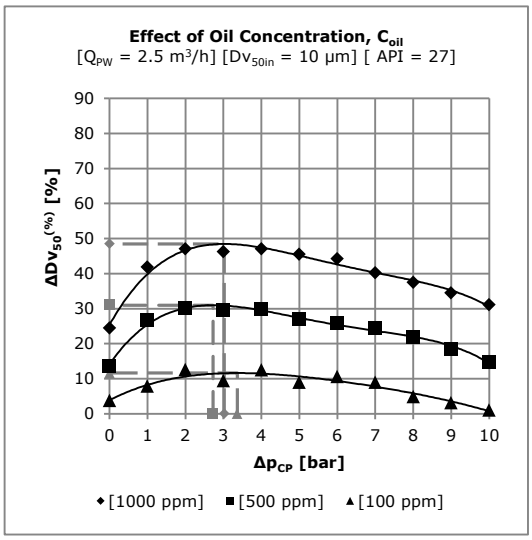

Figure 10 – Percentage change of Dv_{50} ($\Delta Dv_{50}^{(\%)}$) with respect to the pumping pressure (Δp_{CP}) for different oil concentrations (C_{oil}).
Dv_{50in} = 10 µm, Q_{PW} = 2.5 m^3/h, $C_{oil} \in$ {100, 500, 1000}ppm and °API = 27.

The results reveal that a variation in C_{oil} also affects $\Delta Dv_{50}^{(\%)}$. It is seen that an increased C_{oil} leads to an increased $\Delta Dv_{50}^{(\%)}$, regardless of Δp_{CP}. Again, the difference in the coalescing effect is most likely attributed to the difference in droplet collision frequency (Eq. 1) and thereby the coalescence activity, as an increased C_{oil} increases the number of droplets for a constant Dv_{50in}. This trend is observed for both crude oils. For C_{oil} = 500 and C_{oil} = 1000 ppm, a higher $\Delta Dv_{50}^{(\%)}$ was found for the light crude compared to the medium crude. It is also observed that the optimal pumping pressure barely shifts when C_{oil} is changed.

Figure 9 shows that a reduction in C_{oil} from 500 ppm to 100 ppm, while Δp_{CP} = 4 bar, reduced $\Delta Dv_{50}^{(\%)}$ from approximately 50% to under 15%. However, for both conditions, Δp_{CP} = 4 bar is the optimal pumping pressure, and no adjustment of the point of operation is therefore needed.

5.5 Optimal Point of Operation

In Section 5.2, it was observed that the point of operation affected the coalescing effect of the pump. At constant water characteristics, the most beneficial combinations of flow rate and pumping pressure, with respect to the percentage change of Dv_{50}, was found and referred to as the optimal points of operation. The results discussed in Section 5.3 and 5.4 showed how various water characteristics affected the coalescing effect.

In a produced water treatment plant, the upstream process determines the water characteristics. The droplet size distribution and oil concentration at the pump inlet may vary. As seen in the previous investigations, this can affect whether the overall droplet behaviour in the pump is dominated by droplet break-up or droplet coalescence. If, however, the operational point of the pump is continuously adjusted, the coalescing effect can be maximised. Allowing for adjustments in the operating point with respect to the coalescing effect may have significant advantages. For instance, for the conditions in Figure 7 where Dv_{50in} = 5 µm, if Δp_{CP} is increased from 2 bar to 7 bar, $\Delta Dv_{50}^{(\%)}$ is increased from approximately 90% to almost 120%. Similarly, for the conditions in Figure 8 when Dv_{50in} = 15 µm, if Δp_{CP} is reduced from 9 bar to 2 bar, $\Delta Dv_{50}^{(\%)}$ is increased from approximately -10% to almost 20%. In this case, the reduction of Δp_{CP} is critical, as the overall droplet behaviour changes from droplet break-up to droplet coalescence.

In a typical produced water process there are possibilities to change the point of operation as long as the changes are kept within boundaries determined by the overall process plant. If the pumping pressure is allowed to vary, valves downstream from the separation equipment can be used to compensate for the pressure changes. This setup allows for changes to be done with only local influence. Finally, this means that the pump can be considered as a component that increases not only the process pressure but also the separation efficiency of the downstream equipment.

6 CONCLUSIONS

In this paper, the coalescing effect of a newly developed multistage centrifugal pump was investigated. The results show that the coalescing effect is affected by water characteristics, such as the inlet droplet size distribution, oil type, and oil concentration. In addition, the coalescing effect was found to be affected by the point of operation, meaning the pumping pressure with respect to the flow rate. For the investigated combinations of water characteristics and flow rate, an optimal pumping pressure was always found within the pump pressure range. The optimal point of operation is assumed to promote the most beneficial combination of turbulent droplet coalescence and droplet break-up. From an operational point of view, this means that the pump can be considered as a component that increases not only the process pressure but also the separation efficiency of the downstream equipment. Further, if the operating point of the pump is allowed to vary, it can be adjusted with respect to the separation efficiency of the downstream equipment and thereby maximising the potential of the pump.

7 NOTATION

API	American Petroleum Institute
C_{oil}	Oil Concentration
DP	Differential Pressure Transmitter
Dv_{50}	Volume Median Droplet Diameter
Dv_{50in}	Dv_{50} at the Pump Inlet
d	Droplet Diameter
d_{max}	Maximum Stable Droplet Diameter
$\hat{d}_{max}$	Normalised d_{max}
FT	Flow Transmitter
HV	Hand Valve
LT	Level Transmitter
n	Number of Droplets
P	Pump
PCV	Pressure Control Valve
ppm	Parts Per Million
PT	Pressure Transmitter
Q_m	Oil/Water Mixture Flow Rate
Q_{PW}	Produced Water Flow Rate
T	Tank
TT	Temperature Transmitter
V_{VOLUTE}	Volute Volume
We_{CRIT}	Critical Weber Number
$\Delta Dv_{50}^{(\%)}$	Percentage Change of Dv_{50}
Δp	Pumping Pressure
Δp_{CP}	Δp of the Coalescing Pump
ε	Energy Dissipation Rate per Unit Mass
$\hat{\varepsilon}$	Normalised ε
κ	Proportional Constant
μ_D	Viscosity of the Dispersed Phase
ρ_c	Density of the Continuous Phase
ρ_m	Oil/Water Mixture Density
σ	Interfacial Tension
ω_{col}	Collision Frequency

8 REFERENCES

[1] F. R. Ahmadun, A. Pendashteh, L. C. Abdullah, D. R. A. Biak, S. S. Madaeni and Z. Z. Abidin, "Review of technologies for oil and gas produced water treatment," *Journal of Hazardous Materials,* pp. 530 - 551, 19 May 2009.

[2] Petroleum Safety Authority Norway, "Regulations Relating to Conducting Petroleum Activites (The Activities Regulations)," 2015.

[3] T. Husveg, Operational Control of Deoiling Hydrocyclones and Cyclones for Petroleum Flow Control, Stavanger: University of Stavanger, 2007.

[4] S. Judd, H. Qiblawey, M. Al-Marri, C. Clarkin, S. Watson, A. Ahmed and S. Bach, "The size and performance of offshore produced water oil-removal technologies for reinjection," *Separation and Purification Technology,* pp. 241 - 246, 29 July 2014.

[5] A. B. Sinker, M. Humphris and N. Wayth, "Enhanced Deoiling Hydrocyclone Performance without Resorting to Chemicals," *Proceedings of the 1999 Offshore Europe Conference,* pp. 1 - 9, 7 - 9 September 1999.

[6] J. C. Ditria and M. E. Hoyack, "The Separation of Solids and Liquids With Hydrocyclone-Based Technology for Water Treatment and Crude Processing," *Presented at the SPE Asia Pacific Oil and Gas Conference,* pp. 691 - 706, 7 - 10 November 1994.

[7] D. A. Flanigan, M. E. Scribner, J. E. Stolhand and E. Shimoda, "Droplet Size Analysis: A New Tool for Improving Oilfield Separations," *SPE Annual Technical Conference and Exhibition,* 2-5 October 1988.

[8] M. F. Schubert, "Advancements in Liquid Hydrocyclone Separation Systems," *OTC 6869, presented at the 24th Annual OTC,* pp. 497 - 506, 4 - 7 May 1992.

[9] N. van Teeffelen, *Development of a New Separation Friendly Centrifugal Pump,* Stavanger: Presented at Tekna Produced Water Management, 2015.

[10] M. van der Zande, Droplet Break-Up in Turbulent Oil-in-Water Flow Through a Restriction, Delft, the Netherlands: PhD thesis, Delft University of Technology, 2000.

[11] J. M. Walsh, "The Savvy Separator Series: Part 5. The Effect of Shear on Produced Water Treatment," *Oil and Gas Facilities, Volume 5, Number 1,* pp. 16 - 23, February 2016.

[12] S. Ceylan, G. Kelbaliyev and K. Ceylan, "Estimation of the maximum stable drop sizes, coalescence frequencies and the size distributions in isotropic turbulent dispersions," *Colloids and Surfaces A: Physicochemical and Engineering Aspects,* p. 285–295, 23 January 2003.

[13] R. Morales, E. Pereyra, S. Wang and O. Shoham, "Droplet Formation Through Centrifugal Pumps for Oil-in-Water Dispersions," *SPE Journal,* pp. 172-178, February 2013.

[14] Gilson, "305/306 HPLC Pumps Spec Sheet," 2004. [Online]. Available: http://www.gilson.com/Resources/305306_HPLC_Pumps_Spec_Sheet.pdf. [Accessed 15 Mars 2016].

[15] M. J. van der Zande, K. R. van Heuven, J. H. Muntinga and W. M. G. T. van den Broek, "Effect of Flow Through a Choke Valve on Emulsion Stability," *proceedings of SPE Annual Technical Conference and Exhibition,* pp. 1-8, 3-6 October 1999.

[16] T. Husveg, "Centrifugal pump with coalescing effect, design method and use thereof". Patent WO 2014106635 A1, 10 July 2014.

[17] Malvern Instruments Ltd., *RTSizer and Insitec analyser User Manual,* Worcestershire: Malvern Instruments Ltd., 2010.

[18] J. M. Walsh, "Produced-Water-Treatment Systems: Comparison of North Sea and Deepwater Gulf of Mexico," *Oil and Gas Facilities,* pp. 73 - 86, April 2015.